Author Manuscript

Author Manuscript

Author Manuscript

Author Manuscript

HHS Public Access

Author manuscript

Mol Cancer Res. Author manuscript; available in PMC 2019 April 01.

Published in final edited form as:

Mol Cancer Res. 2018 April ; 16(4): 707–719. doi:10.1158/1541-7786.MCR-17-0598.

Cancer Stem Cell Phenotypes in ER+ Breast Cancer Models are Promoted by PELP1/AIB1 Complexes

Thu H. Truong[1], **Hsiangyu Hu**[1], **Nuri A. Temiz**[4], **Kyla M. Hagen**[1], **Brian J. Girard**[1], **Nicholas J. Brady**[1], **Kathryn L. Schwertfeger**[3], **Carol A. Lange**[1,2,*], and **Julie H. Ostrander**[1,*]

[1]Department of Medicine (Division of Hematology, Oncology, and Transplantation), University of Minnesota, Minneapolis MN 55455

[2]Department of Pharmacology, Masonic Cancer Center, University of Minnesota, Minneapolis MN 55455

[3]Department of Laboratory Medicine and Pathology, Masonic Cancer Center, University of Minnesota, Minneapolis MN 55455

[4]Masonic Cancer Center, Institute for Health Informatics, University of Minnesota, Minneapolis MN 55455

Abstract

Proline, glutamic acid, and leucine rich protein 1 (PELP1) is overexpressed in approximately 80% of invasive breast tumors. PELP1 dynamically shuttles between the nucleus and cytoplasm, but is primarily nuclear in normal breast tissue. However, altered localization of PELP1 to the cytoplasm is an oncogenic event that promotes breast cancer initiation and progression. Herein, interacting partners unique to cytoplasmic PELP1 and the mechanisms by which these interactions promote oncogenic PELP1 signaling were sought. AIB1 (amplified in breast cancer 1; also known as SRC-3 or NCOA3) was identified as a novel binding partner of cytoplasmic PELP1 in both estrogen receptor-positive (ER+) and ER-negative cell lines. Cytoplasmic PELP1 expression elevated basal phosphorylation levels (i.e. activation) of AIB1 at Thr24, enhanced ALDH+ tumorsphere formation, and upregulated specific target genes independently of hormone stimulation. Direct manipulation of AIB1 levels using shRNA abrogated cytoplasmic PELP1-induced tumorsphere formation and down-regulated cytoplasmic PELP1-specific target genes. SI-2, an AIB1 inhibitor, limited the PELP1/AIB1 interaction and decreased cytoplasmic PELP1-induced tumorsphere formation. Similar results were observed in a murine-derived MMTV-AIB1 tumor cell line. Furthermore, in vivo syngeneic tumor studies revealed that PELP1 knockdown resulted in increased survival of tumor-bearing mice as compared to mice injected with control cells.

Corresponding Authors: Carol A. Lange (lange047@umn.edu) and Julie H. Ostrander (hans1354@umn.edu).
*Denotes co-principal investigators

Conflict of Interest Statement: The authors declare no potential conflicts of interest

Author Manuscript Author Manuscript Author Manuscript Author Manuscript

INTRODUCTION

Luminal breast cancers account for ~75% of newly diagnosed cases of breast cancer and express estrogen receptor (ER) as well as a range of progesterone receptor (PR)-positive cells. Adjuvant hormone therapies targeting ER actions improve overall survival (1). However, approximately 40% of luminal breast tumors eventually progress to ER+, endocrine-independent disease (2). Mechanisms of resistance to ER-targeted therapies include upregulation and activation of growth factor receptor (GFR) signaling pathways, ER mutations, and upregulation of ER coactivator proteins (3). GFR signaling enhances phosphorylation of ER and ER pathway components, promotes ER cytoplasmic signaling, and ultimately results in profoundly altered gene expression (4–6). To prevent luminal breast cancer recurrence, we need to understand the molecular mechanisms that drive disease progression and identify new biomarkers that can be targeted in combination with ER-targeted therapies.

A promising biomarker for targeting breast cancer progression is PELP1 (proline, glutamic acid, and leucine rich protein 1) (7,8). PELP1 is primarily located in the nucleus (9) in mammary epithelial cells where it serves as a co-activator to a number of transcription factors including steroid hormone receptors (SR) (e.g. ER) and is involved in chromatin remodeling (7), RNA processing (10), and ribosome biogenesis (10). PELP1 expression is dysregulated in many different cancers (e.g. endometrial, ovarian, prostate, brain) and is overexpressed in over 80% of invasive breast tumors (11). High PELP1 expression is associated with tumor grade, tumor proliferation, node-positive invasive breast cancer and distant metastasis, and decreased breast cancer-specific survival and disease-free survival (11–13). Additionally, several studies have shown that PELP1 influences cancer cell biology through mediating changes in proliferation, apoptosis, autophagy, migration, invasion, metastasis, and endocrine resistance (7). Our group demonstrated that both ER and PR form a functional signaling and transcriptional complex with PELP1 to regulate novel estrogen-regulated ER/PR/PELP1-target genes associated with breast cancer progression (14).

PELP1 has also been shown to have cytoplasmic functions. For example, PELP1 acts as a scaffolding protein for growth factor and SRs that modulate cytoplasmic kinase signaling. Altered localization of PELP1 to the cytoplasm was observed in 50% of PELP1-positive breast tumors (9). In preclinical models of breast cancer, overexpression of cytoplasmic PELP1 through mutation of its nuclear localization signal promotes increased activation of cytoplasmic kinase signaling and confers tamoxifen resistance (9). Moreover, expression of cytoplasmic PELP1 in a mammary-specific transgenic mouse model induced mammary gland hyperplasia associated with increased proliferation and pro-survival signaling (i.e., PI3K/Akt and Ras/ERK) (12,15). Analysis of PELP1 localization from tumor samples revealed that patients with high levels of cytoplasmic PELP1 were less likely to respond to tamoxifen than patients with low cytoplasmic PELP1 levels (12). Additionally, our group demonstrated that cytoplasmic PELP1 staining was observed in 36% (4 of 11) of atypical breast needle aspirate samples from women at high risk for developing breast cancer (16). Further, we showed that cytoplasmic PELP1 expression up-regulates pro-tumorigenic IKKε and inflammatory signals that drive a migratory phenotype associated with breast cancer initiation (17). Collectively, these findings in breast cancer cell models, mammary mouse

Author Manuscript Author Manuscript Author Manuscript Author Manuscript

models, and patient samples demonstrate that altered PELP1 localization to the cytoplasm is an oncogenic event that promotes breast cancer initiation and progression. However, the mechanisms by which cytoplasmic PELP1 promotes oncogenesis are still not clearly defined.

Herein, we sought to identify interacting partners unique to cytoplasmic PELP1 and determine whether they promote oncogenic signaling in breast cancer progression. We identified AIB1 (amplified in breast cancer 1; also known as SRC-3 [steroid receptor co-activator 3] or NCOA3 [nuclear receptor co-activator 3]) as a novel binding partner of cytoplasmic PELP1. We found that cytoplasmic PELP1 expression elevated basal Thr24 phosphorylation levels of AIB1 and increased primary and secondary tumorsphere formation in both the presence and absence of estrogen. Estrogen was not required for upregulation of cytoplasmic PELP1-specific target genes associated with cell survival and cancer stem cell biology. Direct manipulation of AIB1 levels using shRNA down-regulated cytoplasmic PELP1-specific target genes and inhibited cytoplasmic PELP1-induced tumorsphere formation. Moreover, knockdown of PELP1 in an AIB1-mouse derived tumor cell line reduced tumorsphere formation *in vitro* and led to increased survival of recipient tumor-bearing mice as compared to control mice. Taken together, our data demonstrate that cytoplasmic PELP1 interacts with AIB1 to drive estrogen-independent events involved in regulation of breast cancer stem cell biology and disease progression.

MATERIALS AND METHODS

General Reagents

Estradiol (E2; Sigma) and hydrocortisone (Sigma) stocks were prepared in ethanol (EtOH). Epidermal growth factor (EGF; Sigma) was prepared in 0.1% BSA containing 10 mM acetic acid. SI-2 stocks were prepared in DMSO (kindly provided by David Lonard, Baylor College of Medicine).

Cell Culture

MCF-7 cells were a gift from Deepali Sachdev (University of Minnesota). STR authentication was performed January 2012 by the Johns Hopkins CORE facility. MCF7 cells were cultured in modified IMEM (Life Technologies) containing 5% FBS (Thermo Scientific HyClone), 1% penicillin-streptomycin (Life Technologies), and 67.5 ng/ml insulin (Life Technologies). T47D CO cells were cultured in MEM (Corning) containing 5% FBS, 1% penicillin-streptomycin, 1% MEM non-essential amino acids (Life Technologies), and 6 ng/ml insulin. Mammary epithelial cells (HMEC-hTERT, MCF10A) were cultured as previously described (16,17). HMECs were purchased from Lonza and MCF-10A cells were purchased from ATCC. For experiments with E2, cells were hormone-starved in phenol-free modified IMEM containing 5% DCC (dextran coated charcoal-stripped FBS; HyClone) for 16 h prior to treatment. J110 cells were a gift from Myles Brown (Dana Farber Cancer Institute) and cultured in DMEM/F-12 (Corning) containing 5% FBS, 5 μg/ml insulin, and 0.1 μg/mL hydrocortisone. All cell lines were tested for mycoplasma prior to the initiation of experiments.

Author Manuscript Author Manuscript Author Manuscript Author Manuscript

Stable Cell Line Generation

MCF-7 cells were transfected per manufacturer's instructions with human specific PELP1 double nickase constructs (sc-405376-NIC-2; Santa Cruz Biotechnology) to knockdown endogenous PELP1 (h2 MCF-7). Stable h2 MCF-7 PELP1 models were generated by transducing h2 MCF-7 cells with retroviral LXSN (which also served as vector control) containing WT PELP1 or cytoplasmic PELP1. Cells were selected in and maintained as described above with 0.5 mg/ml G418 sulfate (Corning). Single cell cloning was used to generate clonal cell lines expressing LXSN, WT PELP1, or cytoplasmic PELP1. Stable shAIB1 (clone TRCN0000365196)-expressing cell lines were created by transducing h2 MCF-7 PELP1 models with pLKO.1 lentiviral vectors containing target gene shRNA sequences from the MISSION TRC library (Sigma). Stable pooled populations were selected in and maintained as described above with 0.5 mg/ml G418 sulfate and 0.5 μg/ml puromycin (MP Biomedicals). To generate J110 PELP1 knockdown cells (PELP1-low), J110 cells were transfected with murine specific PELP1 double nickase constructs (sc-429042-NIC; Santa Cruz Biotechnology) per manufacturer's instructions. Cells were selected for with puromycin and sorted for GFP-positivity by FACS.

Cell Lysate Preparation

Cells were harvested in RIPA-lite lysis buffer [150 mM NaCl, 6 mM Na_2HPO_4, 4 mM NaH_2PO_4, 2 mM EDTA, 100 mM NaF, 1% Triton-X 100, 1× complete mini protease inhibitors (Roche), 1× PhosSTOP (Roche), and supplemented with 1 mM PMSF, 5 mM NaF, 0.05 mM Na_3VO_4, 25 mM beta glycerophosphate (BGP), and 20 μg/ml aprotinin]. For cellular fractionation, cells were harvested using the NE-PER Nuclear and Cytoplasmic Extraction Kit (Thermo Scientific).

TAP-tagged Mass Spectrometry

Interplay Adenoviral TAP system (Agilent) was used for adenoviral expression of TAP-tagged WT PELP1 and cytoplasmic PELP1. WT PELP1 and cytoplasmic PELP1 (NLS mutation) were subcloned into the pNTAP-A shuttle vector to create N-terminal TAP-PELP1 fusion. The pNTAP shuttle vectors were recombined with pADEasy, and the recombinant DNA was linearized and transfected into AD-293 cells for adenoviral production of TAP-CAT (control), TAP-WT PELP1 and TAP-cytoplasmic PELP1. hMEC-hTERT cells were infected with adenovirus for 48 h and then subjected to cellular fractionation. Cytoplasmic extract from hMEC-hTERT cells expressing cytoplasmic-PELP1 or TAP-CAT and nuclear extract from hMEC-hTERT cells expressing WT PELP1 or TAP-CAT were processed through the TAP purification protocol per manufacturer's instructions. Purified protein complexes were separated by SDS-PAGE. Unique bands present only in the cytoplasmic PELP1 cytoplasmic extract or the WT PELP1 nuclear extract were identified by mass spectrometry by the University of Minnesota Center for Mass Spectrometry and Proteomics.

Co-Immunoprecipitation Assays

Cells were harvested in ELB lysis buffer [50 mM HEPES, 0.1% nonidet P-40 (NP-40), 250 mM NaCl, 5 mM EDTA, 1× complete protease inhibitors (Roche), 1× PhosSTOP (Roche), and supplemented with 1 mM PMSF, 1mM NaF, 0.5 mM Na_3PO_4, 25 mM BGP, and 20

Author Manuscript Author Manuscript Author Manuscript Author Manuscript

μg/ml aprotinin]. 1000 μg lysate (1 mg/ml) were incubated with 1 μg of the indicated antibody (e.g. AIB1 or ER) overnight at 4°C. Immunocomplexes were isolated with protein G agarose (Roche) for an additional 2 h at 4°C. Resin was collected and washed with cold ELB buffer. Immunocomplexes were eluted with sample buffer, resolved by SDS-PAGE, and analyzed by Western blot. For assays with cytoplasmic extract, cells were harvested using the NE-PER Nuclear and Cytoplasmic Extraction Kit. Cytoplasmic extracts were then subjected to co-immunoprecipitation assays as described above.

Immunoblotting

Immunoblotting was performed with the following antibodies: phospho-AIB1 (Thr24, Cell Signaling), AIB1 (5E11, Cell Signaling), β-actin (AC-40, Sigma), phospho-ER (Ser118, Cell Signaling), ER (F-10, Santa Cruz Biotechnology), GAPDH (0411, Santa Cruz Biotechnology), HDAC2 (H-54, Santa Cruz Biotechnology), p65 (F-6, Santa Cruz Biotechnology), PELP1 (A300-180A, Bethyl Labs), goat anti-rabbit IgG-HRP (BioRad), and goat anti-mouse IgG-HRP (BioRad). Blots were developed with ECL using Super Signal West Pico Maximum Sensitivity Substrate (Pierce) and imaged by film.

Real-Time Quantitative-PCR (RT-qPCR)

Total RNA was extracted from cell samples using TriPure Isolation Reagent (Roche) and isopropanol precipitation. RNA (1000 ng) was reverse transcribed to cDNA according to manufacturer's instructions using qScript cDNA SuperMix (Quanta BioSciences). qPCR was performed using Light Cycler FastStart DNA Master SYBR Green I (Roche) on a Light Cycler 480 II Real-Time PCR System (Roche). qPCR cycling conditions were: initial denaturation at 95°C (10 min), denature at 95°C (10 sec), anneal at 60°C (10 sec), and extension at 72°C (5 sec) for 45 cycles. Target gene levels were normalized to standard housekeeper genes (TBP or 18s) and represent the average of three independent measurements (mean ± SD).

RNA-Sequencing

h2 MCF-7 PELP1 cells expressing LXSN, WT PELP1, or cytoplasmic PELP1 were hormone-starved in modified IMEM containing 5% DCC for 16 h prior to hormone treatment. Cells (in triplicate) were treated with vehicle or E2 (10^{-9} M) for 6 h, followed by RNA extraction using an RNeasy Mini Kit (Qiagen). 50 base pair paired-end sequencing was performed at the University of Minnesota Genomics Center using Illumina HiSeq 2500 system. On average over 12 million reads were sequenced per sample. Each sample was aligned using the Tophat aligner (version 2.0.13). Samtools software (version 1.0_BCFTools_HTSLib) was used to sort and index bam files. Cuffquant (Cufflinks version 2.2.1) was used to generate transcript abundance files. Once all samples within each species were mapped and abundance estimate files were completed, Cuffnorm (Cufflinks version 2.2.1) was used to generate a table of Fragments Per Kilobase Of Exon Per Million Fragments Mapped (FPKM) values for genes within each sample. For each gene, fpkm values were log transformed and mean centered. Genes that varied less than 0.5 standard deviation within the sample set were removed from further analysis. A simple t-test with Benjamini-Hochberg correction and a minimum of 1.5-fold change cut-off was used to identify differentially expressed genes between various conditions.

Author Manuscript Author Manuscript Author Manuscript Author Manuscript

Immunofluorescence

Cells were fixed with cold methanol for 10 min at −20 °C, washed with PBS, permeabilized for 15 min in PBS (0.05% Triton X-100; permeabilization solution), and blocked for 30 min in PBS (0.5% Triton X-100, 5% BSA, normal goat IgG [1:500]; blocking solution). Cells were then incubated with rabbit anti-PELP1 primary antibody in blocking solution for 1 h. Cells were washed with PBS and incubated with AlexaFluor488-conjugated goat anti-rabbit (Life Technologies) secondary antibody in blocking solution for 1 h. Cells were washed with PBS, dehydrated using ethanol, and mounted with DAPI containing ProLong Gold anti-fade reagent (Life Technologies).

Soft Agar Assays

Cells were seeded (4×10^4 cells/well) in 1× sterile low melt agarose (Life Technologies) containing 5% DCC and the appropriate treatment (vehicle [EtOH] or E2 [1 nM]). Soft agar assays were allowed to proceed for 21 days at 37 °C. Afterwards, cell colonies were stained with 0.1% crystal violet for 1 h and washed with PBS. Data are presented as the average ± SD of three independent measurements.

Tumorsphere Assays

Adherent cells were washed with PBS and dissociated enzymatically in 0.25% trypsin-EDTA (Invitrogen). Cells were sieved through a 40-μm sieve (BD Falcon). Single cells were plated in ultra-low attachment plates (Corning). Cells were grown in a serum-free mammary epithelial basal medium (MEBM; Lonza) containing 1% methylcellulose (Sigma), 1% B27 supplement (Invitrogen), 1% penicillin-streptomycin, 5 μg/ml insulin, 20 ng/ml EGF, 1 ng/ml hydrocortisone, and 100 μM β-mercaptoethanol. For secondary, primary tumorspheres were collected and dissociated enzymatically in 0.25% trypsin-EDTA. Cells were plated as described above in conditioned media, which consisted of a 1:1 mixture of MEBM media (described above) and media from cultured parental cells. Tumorspheres were allowed to grow for 12 days. Tumorspheres were analyzed by total number, and scored by manual counting using a uniformly scaled grid. Data are presented as the average ± SD of three independent measurements.

Flow Cytometry

An ALDEFLUOR assay kit (Stem Cell Technologies) was used per manufacturer's instructions to assay for aldehyde dehydrogenase (ALDH) activity. Cells were plated in ultra-low attachment plates and grown in MEBM media (described above) to generate tumorspheres. Tumorspheres were collected and dissociated enzymatically in 0.25% trypsin-EDTA. Cells were resuspended (5×10^5) in ALDEFLUOR assay buffer (1 ml). ALDEFLUOR reagent was added to this cell suspension, mixed, and then half of the cell suspension was transferred to a separate tube containing DEAB. The cells were incubated at 37 °C for 45 min, washed, and then subjected to flow cytometry using the BD LSRII H4760 flow cytometer (BD Biosciences).

Author Manuscript Author Manuscript Author Manuscript Author Manuscript

In vivo syngeneic tumor model

Ten mice per group were injected with 5×10^3 J110 (parental or PELP1-low) cells into the right inguinal mammary fat pad of 3–4 week old female FVB mice (Harlan Laboratories). Once palpable tumors were detected, tumors were measured by caliper every 2–3 days. Mice were euthanized once tumors reached 1 cm^3 in size. Differences in survival were analyzed using Kaplan–Meier methodology and curves compared using the Mantel–Cox log-rank test. Animal studies were reviewed and approved by the University of Minnesota Institutional Animal Care and Use Committee (IACUC).

Statistical Analysis

Data was tested for normal distribution using Shapiro-Wilks normality test and homogeneity of variances using Bartlett's Test. Once data were determined to meet these two requirements, statistical analyses were performed using one-way ANOVA in conjunction with Tukey multiple comparison test for means between more than two groups or Student *t* test for means between two groups, where significance was determined with 95% confidence.

RESULTS

AIB1 interacts with cytoplasmic PELP1 in human mammary epithelial cells

To identify proteins that may participate in oncogenic PELP1 signaling (i.e. cytoplasmic PELP1) during breast cancer progression, we expressed tandem affinity purification (TAP)-tagged PELP1 constructs in hMEC-hTERT cells, a model of normal human mammary epithelial cells (hMECs). Following adenovirus transduction of hMEC-hTERT cells with TAP-WT PELP1, TAP-cyto PELP1, or TAP-CAT (control), cell lysates were subjected to cellular fractionation, processed through the TAP protocol to purify cytoplasmic or nuclear TAP-PELP1 complexes, and separated using SDS-PAGE; bands of interest were analyzed by mass spectrometry. The mass spectrometry results are summarized in Supplementary Table 1. Pathway analysis (IPA and KEGG) was performed for both cytoplasmic (Supplementary Table 2) and nuclear extracts (Supplementary Table 3). Pathways of interest that were identified from the cytoplasmic interacting proteins by IPA included 'Cancer', 'Cellular Movement' and 'Cell Cycle' pathways. The top pathway identified by KEGG analysis of PELP1 nuclear interacting proteins was 'Ribosome biogenesis in eukaryotes', a known PELP1 nuclear function (10). Interestingly, AIB1 (also known as SRC-3 or NCOA3) was identified only in the cytoplasmic protein extract. The *AIB1* gene locus is amplified ~10% in breast and ovarian cancer and overexpressed ~60% in breast tumors (18). Similar to PELP1, AIB1 functions as a SR co-activator, is a critical member of hormone-responsive transcriptional machinery (19), and is a known driver of oncogenic phenotypes associated with luminal breast cancer progression (20,21).

Given the clear relevance of AIB1 in breast cancer biology (22) and functional overlap between AIB1 and PELP1, we chose to further probe the relationship between these two co-activators. We first confirmed the results from our TAP-tagged mass spectrometry analysis by performing the TAP pull-down of cytoplasmic PELP1 from whole cell extracts and then immunoblotting for co-purified AIB1 (Figure 1A); AIB1 and cytoplasmic PELP1 readily

Author Manuscript Author Manuscript Author Manuscript Author Manuscript

interact in TAP pull-down samples. Additionally, we assessed AIB1's interaction with cytoplasmic PELP1 (i.e. untagged) in previously described MCF10A cells (17), an hMEC model engineered to stably express LXSN (vector control) or cytoplasmic PELP1. Immunoprecipitation of AIB1 confirmed increased association between AIB1 and PELP1 in cells expressing cytoplasmic PELP1 relative to LXSN (Figure 1B). These results confirm the findings from our TAP-tag mass spectrometry approach and demonstrate that AIB1 interacts with cytoplasmic PELP1 independently of the TAP-tag in hMECs.

Generation of SR+ breast cancer cell models of cytoplasmic PELP1

Models of normal mammary epithelial cells contain low SR levels and, in general, are SR negative. Our prior work demonstrated that both ER and PR-B form a functional signaling and transcriptional complex with PELP1 to regulate novel ER/PR/PELP1 target genes associated with endocrine resistance (14). Growth factor-induced activation of cytoplasmic kinases enhances SR phosphorylation and transcriptional activation (5,6,23). Namely, cytoplasmic PELP1 links growth factor signaling to highly efficient ER phosphorylation and activation (9). To study the impact of cytoplasmic PELP1 and AIB1 in the context of SR function, we sought to generate PELP1 knock-down and add-back models of SR+ breast cancer cells. We first screened a panel of known SR+ luminal breast cancer cells for high expression of AIB1 and PELP1. MCF-7, BT-474, ZR-75, and T47D CO breast cancer lines were chosen on the basis of their known increased SR expression (i.e. ER and PR) (24). Additionally, MCF-7 and BT-474 cells are known to have AIB1 gene amplification (18). T47D CO is a T47D variant cell line that contains both ER and PR, wherein PR is constitutively expressed (25). Notably, basal mRNA (Figure 2A) and protein (Supplementary Figure 1A) expression levels suggest that PELP1 and AIB1 may be co-expressed in ER+ breast cancer cells. MCF-7 cells were chosen for further study based on their high expression of ER, PR, AIB1, and PELP1 (24). To reduce endogenous PELP1 expression in parental MCF-7 cells, we employed a double nickase approach to target endogenous PELP1 (Figure 2B; h2 MCF-7). These PELP1 knockdown cells will be referred to as h2 MCF-7 cells. h2 MCF-7 cells were then engineered to stably express LXSN (vector control), WT PELP1, or cytoplasmic PELP1 by retroviral transduction (Figure 2C; h2 MCF-7 PELP1). To generate cells stably expressing cytoplasmic PELP1, we mutated the PELP1 nuclear localization signal (KKLK → EELE; cytoplasmic PELP1 NLS mutant) as previously reported (9,16). Analysis of protein (Figure 2C) and mRNA (Supplementary Figure 1B) levels demonstrated successful overexpression of both WT and cytoplasmic PELP1. Of note, despite significant PELP1 mRNA and protein knockdown, we were unable to completely knockout PELP1 expression; hence, a slight band representing endogenous PELP1 is observed in LXSN whole cell lysates (Figure 2C) and nuclear extracts (Figure 2D). Similar results were observed upon PELP1 knockout via CRISPR-based technology in additional breast cancer cell lines, suggesting that PELP1 nuclear functions are required for cell viability. Importantly, PELP1 dynamically shuttles between the cytoplasm and nucleus. The NLS mutation decreases the rate of nuclear translocation and thus increases steady state levels of PELP1 in the cytoplasm. We further characterized h2 MCF-7 PELP1 cells via cellular fractionation (Figure 2D) and immunofluorescence (Figure 2E). As we predicted, signal is observed in both the nuclear and cytoplasmic fractions in cells stably overexpressing either WT or cytoplasmic PELP1. Western blotting of cytoplasmic and

Author Manuscript Author Manuscript Author Manuscript Author Manuscript

nuclear extracts confirmed that WT PELP1 is primarily located in the nucleus, whereas a larger fraction of cytoplasmic PELP1 is localized to the cytoplasm in the respective models (Figure 2D). Similar results were observed in intact cells stained for PELP1 via immunofluorescence (Figure 2E). Additionally, we performed co-immunoprecipitation experiments in h2 MCF-7 PELP1 cells. We consistently observed increased interaction between AIB1 and PELP1 in cells expressing cytoplasmic PELP1 relative to either WT PELP1 or LXSN (Figure 2F, from whole cell lysates; Figure 2G, from cytoplasmic extracts) under basal conditions. Similarly, enhanced interaction between ER and PELP1 occurred in cells expressing cytoplasmic PELP1 (Figure 2H; basal conditions). The interaction between ER and AIB1 as detected in co-IPs was also increased in cells expressing cytoplasmic PELP1 (Figure 2I; basal conditions). Collectively, characterization of h2 MCF-7 PELP1 cells confirms overexpression of predominately nuclear (WT PELP1) or cytoplasmic (cytoplasmic PELP1 NLS mutant) PELP1, and corroborates our finding that AIB1 is a novel preferential binding partner of cytoplasmic PELP1 in multiple cell lines. Moreover, expression of cytoplasmic PELP1 has a direct effect on other protein-protein interactions such as AIB1 co-association with ER in SR+ breast cancer models.

AIB1 phosphorylation at Thr24 is increased in cells expressing cytoplasmic PELP1

Previous studies have shown that cytoplasmic phosphorylation of AIB1 is required for its nuclear translocation and function as a coactivator of transcription (19,26). We predicted that AIB1 phosphorylation levels may be altered as a result of its enhanced interaction with cytoplasmic PELP1. Therefore, we analyzed basal levels of AIB1 Thr24 phosphorylation in multiple cell models (normal and cancer) expressing cytoplasmic PELP1. Consistent with the role of cytoplasmic AIB1 phosphorylation as a required step for nuclear activation, cellular fractionation studies revealed that Thr24 phosphorylation levels of AIB1 were increased in the nuclear fractions of both MCF10A (Figure 3A) and T47D CO (Figure 3B) cells overexpressing cytoplasmic PELP1 relative to LXSN or WT PELP1. Notably, basal levels of AIB1 Thr24 phosphorylation in h2 MCF-7 cytoplasmic PELP1 cells were increased in the cytoplasmic fraction relative to LXSN and WT PELP1 cells (Figure 3C; left); however, due to high levels of phosphorylated Thr24 AIB1 in the nuclear fractions of all h2 MCF-7 PELP1 cell lines, we were unable to detect PELP1-induced changes in nuclear AIB1 Thr24 phosphorylation. Interestingly, estrogen (E2) treatment had no effect on AIB1 Thr24 phosphorylation over vehicle control (Supplementary Figure 2). These results indicate that AIB1 Thr24 phosphorylation (i.e. a molecular marker of nuclear activation) is increased in multiple models expressing cytoplasmic PELP1.

Cytoplasmic PELP1 expression induced changes in global gene expression

Previous global gene expression analysis in SR-negative hMEC-hTERT PELP1 models revealed upregulation of NF-κB-regulated genes involved in inflammation (e.g. *IL-8, CXCL1, IL-1β*; (17)). However, we did not observe similar cytoplasmic PELP1-induced changes in the expression of inflammatory mediators in SR+ h2 MCF-7 PELP1 models. These results suggest that cytoplasmic PELP1 signaling is significantly different in SR+ versus SR− cell lines and that other pathways are modulated by cytoplasmic PELP1 in SR+ breast cancer. To further elucidate pathways altered by cytoplasmic PELP1 in SR+ breast cancer cells, we performed an RNA-Seq analysis in h2 MCF-7 PELP1 models. h2 MCF-7

Author Manuscript Author Manuscript Author Manuscript Author Manuscript

PELP1 cells stably expressing LXSN, WT PELP1, or cytoplasmic PELP1 were treated with vehicle (EtOH) or E2 for 6 h, and RNA was isolated and subjected to RNA-Seq analysis as described in *Methods*.

Differentially expressed genes were identified between WT PELP1 or cyto PELP1 h2 MCF-7 cells (≥ 1.5-fold, Benjamini-Hochberg $q < 0.05$, hierarchical clustering; Figure 4A). Cytoplasmic PELP1 expressing cells had 39 genes differentially expressed genes compared to WT PELP1 in vehicle conditions (17 up-regulated, 22 down-regulated) and 57 differentially expressed genes compared to WT PELP1 in E2 conditions (23 up-regulated, 34 down-regulated). Ingenuity Pathway analysis (IPA) was performed for cyto PELP1 vs. WT PELP1 for vehicle (Supplementary Table 4) and E2 conditions (Supplementary Table 5). Genes known to be involved in cancer biology were pursued further. *AMIGO2*, *NELL2*, and *HAPLN1* were chosen for their involvement in cell survival and stem/progenitor cell formation. Cytoplasmic PELP1-induced expression of these genes was confirmed by quantitative (q)RT-PCR validation (Figure 4B). Additionally, *SERPINE1*, which encodes for PAI-1, is elevated in breast tumor tissues and is correlated with reduced response to tamoxifen (27,28), was found to be upregulated by cytoplasmic PELP1 but failed to meet the 1.5-fold cut off for inclusion in the heat-map (Figure 4A). Upon query of the Kaplan-Meier Plotter breast cancer database (29), we found that *AMIGO2* expression is associated with a decrease in progression-free survival (PFS) in patients with ER+ breast cancer (Supplementary Figure 3A), and that *SERPINE1* expression is associated with a decrease in PFS regardless of ER status (Supplementary Figure 3B, 3C). In summary, genes associated with advanced breast cancer biology were upregulated in SR+ breast cancer cells expressing cytoplasmic PELP1 as compared to cells expressing LXSN or WT PELP1, as demonstrated by RNA-Seq analysis and qRT-PCR validation experiments.

Cytoplasmic PELP1 expression inhibits anchorage-independent proliferation, but enhances cancer stem cell outgrowth

Based on the results of the RNA-Seq studies indicating that cytoplasmic PELP1 is promoting advanced breast cancer biology, we initially performed soft agar colony formation assays to examine effects on cell survival and proliferation in an anchorage independent environment. h2 MCF-7 PELP1 cells were cultured in hormone-free starvation media in the presence of vehicle or E2 (1 nM). Soft agar analysis revealed no differences between LXSN, WT PELP1, or cytoplasmic PELP1 with respect to total number of colonies (Figure 5A); however, there was a ~2-fold decrease in average colony size among cytoplasmic PELP1-expressing cells as compared to cells expressing either LXSN or WT PELP1 (Figure 5B; $p < 0.0001$, Supplementary Figure 4). Further, E2 treatment had no effect on total number of colonies (Figure 5A) or colony size (Figure 5B). These results indicate that cytoplasmic PELP1 expression attenuates proliferation as indicated by colony size, but does not alter cell survival as indicated by colony number in anchorage-independent growth assays.

Proliferative pathways often oppose pathways involved in stem cell expansion or EMT programs (30–32). Based on our observation that cytoplasmic PELP1 inhibited proliferation, but not survival, in anchorage-independent growth assays (Figure 5B), we tested whether

Author Manuscript Author Manuscript Author Manuscript Author Manuscript

cytoplasmic PELP1 expression affected cancer stem cell phenotypes. Tumorsphere assays assess the ability of a minority population of breast cancer stem cells to expand in suspension culture (33). We performed tumorsphere assays (primary and secondary) using h2 MCF-7 PELP1 cells stably expressing LXSN (control), WT PELP1, or cytoplasmic PELP1. Interestingly, cells expressing cytoplasmic PELP1 exhibited a basal increase in primary tumorsphere formation as compared to cells expressing either LXSN or WT PELP1 (Figure 5C; $p = 0.001$). This trend was also observed in E2-treated cells expressing cytoplasmic PELP1; E2 treatment increased the number of primary tumorspheres in all cell lines (Figure 5C). We then performed secondary tumorsphere assays as a functional readout for breast cancer stem cell expansion. Cells expressing cytoplasmic PELP1 cells exhibited increased secondary tumorsphere formation in both the absence and presence of estrogen (Figure 5D). Additionally, enhanced intrinsic aldehyde dehydrogenase (ALDH) activity is a hallmark of cancer stem cells (34). Aldefluor assays confirmed that cells expressing cytoplasmic PELP1 (11.4% ± 1.9) were enriched for ALDH+ activity relative to cells expressing LXSN (6.3% ± 0.56; $p = 0.014$) or WT PELP1 (2.7% ± 0.64; $p = 0.0008$) (Figure 5E, Supplementary Figure 5). These results demonstrate that cytoplasmic PELP1 expression inhibits proliferation as measured by anchorage-independent growth assays, but drives breast cancer stem cell expansion, as measured using secondary tumorsphere assays and ALDH+ activity.

Targeting AIB1 and PELP1 inhibits *in vitro* tumorsphere formation and *in vivo* tumorigenesis

Cytoplasmic PELP1 complexes with AIB1 and mediates increased AIB1 Thr24 phosphorylation/activation. To test the requirement for AIB1 in cytoplasmic PELP1-induced changes in gene expression and associated breast cancer phenotypes, we first transduced h2 MCF-7 PELP1 cells with shRNA (shControl or shAIB1) to knockdown endogenous AIB1. Analysis of AIB1 mRNA (Figure 6A) and protein (Figure 6B) levels demonstrates successful knockdown in h2 MCF-7 PELP1 cells with no effect on PELP1 expression. Cytoplasmic PELP1-regulated genes identified by RNA-Seq (e.g. *AMIGO2*, *NELL2*, *SERPINE1*) were down-regulated upon AIB1 knockdown in cells expressing cytoplasmic PELP1 (Figure 6C). Tumorsphere assays were performed using shAIB1 knockdown cells. Similar to previous results (Figure 5C, 5D), shControl cytoplasmic PELP1 cells exhibited a basal increase in both primary and secondary tumorspheres (Figure 6D, 6E). However, tumorsphere formation was markedly decreased in both primary and secondary tumorspheres derived from shAIB1 knockdown cells relative to shRNA control cells (Figure 6D, 6E). Again, E2 treatment increased primary tumorsphere formation in all cell lines (shControl and shAIB1). However, the E2-induced proliferative effect was greatly attenuated in secondary tumorspheres derived from shAIB1 cell lines. In addition to AIB1 shRNA knockdown, we tested whether pharmacological inhibition of AIB1 would disrupt the cytoplasmic PELP1/AIB1 interaction and block tumorsphere formation. SI-2 is a small molecule inhibitor of AIB1 that has been shown to reduce AIB1 protein levels and thereby inhibit primary tumor growth in mouse models of breast cancer (35). Notably, treatment of SR+ h2-MCF-7-PELP1 cells with 100 nM SI-2 inhibited the cytoplasmic PELP1/AIB1 interaction in co-immunoprecipitation experiments (Figure 6F). To test the effect of SI-2 on tumorsphere formation, h2 MCF-7 PELP1 cells were treated with either SI-1 (100 nM) or

Author Manuscript Author Manuscript Author Manuscript Author Manuscript

vehicle. Interestingly, treatment with SI-2 (Figure 6G) decreased tumorsphere formation in cytoplasmic PELP1-expressing cells, but had little effect on LXSN and WT PELP1 h2 MCF-7 cells. Collectively, these results demonstrate that AIB1 is a key mediator of cytoplasmic PELP1-induced changes in gene expression and associated breast cancer stem cell-like phenotypes.

The mouse mammary tumor virus-AIB1 (MMTV-AIB1) model exhibits mammary gland hyperplasia that progresses to invasive ER+/ER− tumors (36). To evaluate the role of AIB1/PELP1 signaling in an AIB1 tumor model *in vitro* and *in vivo*, we utilized a mouse tumor cell line (J110) established from the MMTV-AIB1 mouse model (37) and employed a double nickase approach to knockdown endogenous PELP1. Although we were unable to completely knockout PELP1, we achieved significant PELP1 knockdown (Figure 7A; PELP-low). Tumorsphere assays demonstrated that J110 PELP1-low cells exhibited reduced tumorsphere formation compared to J110 parental cells (Figure 7B). Additionally, similar to the h2 MCF-7 PELP1 model, SI-2 inhibited tumorsphere formation in J110 parental cells (Figure 7C).

To test the effect of PELP1 knockdown *in vivo*, J110 cells (parental or PELP1-low) were injected into the mammary fat pads of syngeneic FVB mice (10 mice/group). Mice injected with J110 PELP1-low cells exhibited increased median survival relative to mice injected with J110 parental cells (34 vs. 24 days, $p < 0.0001$; Figure 7D). In sum, these results demonstrate that directly targeting PELP1 has the potential to inhibit tumor growth, particularly in the context of AIB1-induced tumorigenesis.

DISCUSSION

Cytoplasmic PELP1 signaling has been implicated in breast cancer initiation and progression (7,17). However, the molecular mechanisms of cytoplasmic PELP1-driven changes in breast cancer biology remain largely unknown. Our study identifies a novel role for AIB1 as a preferential binding partner for cytoplasmic PELP1 in hMEC and breast cancer cell models. In particular, our data demonstrate that cytoplasmic PELP1 overexpression increases Thr24 phosphorylation of AIB1 (an event required for nuclear AIB1 function as a co-activator), upregulates specific target genes, and enhances ALDH+ tumorsphere formation. Knockdown of AIB1 down-regulates cytoplasmic PELP1-specific target genes and inhibits tumorsphere formation. Moreover, knockdown of PELP1 in a tumor cell line derived from AIB1 transgenic mice inhibits *in vitro* tumorsphere formation and *in vivo* tumorigenesis. Taken together, our data identify cytoplasmic PELP1-dependent AIB1 signaling as a key mediator of tumor progression and indicate that the PELP1/AIB1 complex is an important driver of breast cancer stem cell expansion and escape from hormonal regulation.

Functional Parallels Between PELP1 and AIB1

Many similarities exist between PELP1 and AIB1 beyond acting as SR co-activators. For example, AIB1 amplification and overexpression has been shown to promote breast tumor initiation, progression and metastasis (22). Additionally, AIB1 overexpression is linked to endocrine resistance in breast cancer cells and human breast tumors (38–40). Female AIB1

Author Manuscript Author Manuscript Author Manuscript Author Manuscript

transgenic mice develop mammary hyperplasia, similar to cytoplasmic PELP1 transgenic mice (12), which eventually progresses to invasive SR+/SR− tumors (36). Interestingly, increased AIB1 cytoplasmic localization has been reported in breast tumors (36). These diverse studies examined cytoplasmic PELP1 or AIB1 separately, and although there are clear parallels, our findings are the first to mechanistically link PELP1-mediated events to activated AIB1 in breast cancer.

A growing body of evidence implicates AIB1 as a mediator of stem/progenitor cell formation. Relevant to our findings, AIB1 is known to maintain self-renewal in embryonic stem cells (41), drive formation of cancer stem-like cells, and support tumor outgrowth in breast cancer models (42). We show that overexpression of cytoplasmic PELP1 enhances tumorsphere formation in h2 MCF-7 PELP1 models (Figure 5C, 5D); however, this effect is abrogated in response to shRNA-mediated AIB1 knockdown (Figure 6D, 6E). Additionally, Rohira *et al.* demonstrated that SI-2 treatment decreased AIB1-induced cancer stem cell formation in breast cancer and xenograft models (42). We demonstrate that SI-2 treatment in h2 MCF-7 PELP1 models reduced tumorsphere formation in cytoplasmic PELP1 cells (Figure 6G). Our findings support a growing body of evidence that implicates AIB1 as a mediator of stem/progenitor formation and links this event directly to cytoplasmic PELP1 signaling.

Oncogenic PELP1/AIB1 Signaling in SR-Dependent Events

Herein, our findings demonstrate that expression of cytoplasmic PELP1 in h2 MCF-7 PELP1 models enhances SR protein-protein interactions, particularly between cytoplasmic PELP1/ER and AIB1/ER (Figure 2H, 2I). Surprisingly, our RNA-Seq studies did not reveal significant changes in E2-induced gene expression in cells expressing cytoplasmic PELP1 relative to WT PELP1. Instead however, cytoplasmic PELP1 enhanced basal gene expression, which was highly dependent on AIB1 (Figure 6C). Further, cytoplasmic PELP1 expression enhanced basal AIB1 Thr24 phosphorylation in multiple PELP1 breast cell models (Figure 3). Studies have shown that AIB1 must be phosphorylated in the cytoplasm to enable AIB1 co-activator function in the nucleus (19,26). Therefore, the increased binding interaction between cytoplasmic PELP1 and AIB1 observed in our co-immunoprecipitation assays (Figure 1B, 2F) may serve as a mechanism to augment phospho-Thr24 AIB1 activation levels in breast cancer cells, leading to increased AIB1-dependent gene expression.

Our gene expression analyses are consistent with our finding that E2 treatment had little effect on AIB1 Thr24 phosphorylation relative to vehicle controls in cytoplasmic PELP1-expressing cells (Supplementary Figure 2). These data suggest that in the context of luminal breast cancer, cytoplasmic PELP1-induced AIB1 Thr24 phosphorylation and activation may promote the emergence of hormone-independent pathways to SR target gene expression. Further studies are needed to understand how oncogenic PELP1/AIB1 complexes may alter hormonal inputs to SR signaling.

Author Manuscript Author Manuscript Author Manuscript Author Manuscript

PELP1 Target Genes in Breast Cancer

Our RNA-Seq analysis identified target genes of interest related to cell survival, breast tumor progression and stem/progenitor cell formation (*AMIGO2*, *NELL2*, *SERPINE1*, and *HAPLN1*). *AMIGO2*, a cell adhesion molecule, has been shown to modulate cell survival in endothelial cells by directly interacting with PDK1 and facilitating Akt signaling to promote tumor growth and angiogenesis (43). *NELL2* has been shown to mediate increased cell survival in neural cells through trans-activation by ERα and ERβ (44). *SERPINE1* encodes for PAI-1 and belongs to the serpin superfamily of protease inhibitors. PAI-1 is emerging as a prognostic biomarker for breast cancer, and a number of studies suggest that PAI-1 may enhance disease progression by blocking apoptotic pathways and thereby enhancing cell survival (45). Thus, cytoplasmic PELP1 expression may upregulate genes involved in mediating cell survival as a means to promote breast cancer progression. Our studies show that *AMIGO2*, *NELL2* and *SERPINE1* are upregulated in cytoplasmic PELP1-expressing cells and down-regulated in response to AIB1 shRNA-mediated knockdown; these findings suggest these genes are reflective of a cytoplasmic PELP1/AIB1 gene signature.

We also identified a cytoplasmic PELP1-induced gene (*HAPLN1*) relevant to cancer stem cell biology. Mebarki *et al*. demonstrated *de novo HAPLN1* expression occurs in aggressive hepatocellular carcinoma tumors expressing stem cell markers and in *in vitro* models of EMT via the Wnt/β-catenin signaling pathway (46). Considering that cells expressing cytoplasmic PELP1 form increased both tumorsphere formation and intrinsic ALDH activity, we were surprised that our RNA-Seq studies did not identify more genes directly related to cancer stem cell biology. However, breast cancer stem cells represent a small minority of the total cell population (1–5% of MCF-7 cells are cancer stem cells (47)), making it difficult to detect changes in global gene expression by RNA-Seq, particularly when performed on RNA isolated from cells grown in adherent 2D conditions. Future studies will specifically examine gene expression in breast cancer stem cell populations maintained as spheroids (i.e. 3D culture systems) to further identify genes specifically regulated by cytoplasmic PELP1/AIB1 signaling.

PELP1 as a Therapeutic Target in Breast Cancer

PELP1 is emerging as a viable therapeutic target and biomarker for women with breast cancer. Pre-clinical studies illustrate that peptidomimetics and small molecule inhibitors can specifically disrupt PELP1 protein-protein interactions. The PELP1 peptidomimetic inhibitor, D2, is designed to specifically inhibit the PELP1/androgen receptor complex via disruption of LXXLL-mediated protein-protein interactions (48). Our study identifies the PELP1/AIB1 complex as a novel protein-protein interaction that could be selectively targeted by potent inhibitors. Small molecule inhibitors (e.g. SI-2) recently developed for AIB1 have shown pre-clinical utility in breast cancer cell lines and mouse models (35), and here we show that SI-2 inhibits PELP1-induced tumorsphere formation. Others have also shown that targeting the PELP1-interacting proteins KDM1 (49) and mTOR (50) inhibits PELP1-mediated tumor growth. Furthermore, these reports also demonstrate that PELP1 promotes endocrine therapy resistance and inhibition of KDM1 and mTOR sensitizes cells to PELP1-mediated tamoxifen resistance. Acquired resistance to hormone therapy remains a major clinical problem. Therefore, inhibitors capable of selectively targeting cytoplasmic

Author Manuscript Author Manuscript Author Manuscript Author Manuscript

PELP1 interacting partners that promote therapy resistance would provide a means to target luminal breast cancers and could be used in lieu of (or in conjunction with) ER-targeted therapies.

In addition to therapeutic targeting, our studies suggest that cytoplasmic PELP1 and phospho-Thr24 of AIB1 could be used as biomarkers to identify breast cancer patients likely to respond to therapeutic strategies designed to selectively target PELP1, AIB1, or the oncogenic PELP1/AIB1 complex. Our *in vivo* studies (Figure 7) indicate that mice transplanted with AIB1-derived mouse tumor cells with PELP1 knockdown survive longer than mice transplanted with tumor cells expressing PELP1. These studies suggest that manipulating PELP1 location or levels has the potential to mitigate tumor progression, particularly in the context of AIB1-mediated tumorigenesis.

CONCLUSION

Our data suggests a model (Figure 7E) in which cytoplasmic PELP1/AIB1 complexes promote persistently elevated cytoplasmic AIB1 Thr24 phosphorylation. We hypothesize this occurs through PELP1 functioning as a cytoplasmic scaffolding protein that brings together signaling molecules and protein kinases that mediate robust AIB1 Thr24 phosphorylation. AIB1 phosphorylation is known to occur on at least 6 different sites in response to different stimuli (hormones, growth factors, and cytokines), but phospho-specific antibodies are not commercially available for all sites. Thus, it is likely that cytoplasmic PELP1 signaling promotes site-specific Thr24 phosphorylation that directs AIB1 to regulate specific target genes. Future studies will be aimed at identifying PELP1-induced AIB1 phosphorylation sites and the kinase signaling complexes recruited by cytoplasmic PELP1.

Our data also suggests that inhibiting the cytoplasmic PELP1/AIB1 signaling complex may specifically target the breast cancer stem cell population. Breast cancer stem cells are believed to play a key role in breast cancer development, disease progression, and therapy resistance (51). Importantly, these minority populations of pluripotent cells are slow growing and not targeted by standard chemotherapies or endocrine therapies. If we can identify intracellular pathways or molecular complexes that drive survival and expansion of breast cancer stem cells, we would be able to target this sub-population of cancer cells and have the potential to significantly impact on the overall survival of women diagnosed with breast cancer.

Supplementary Material

Refer to Web version on PubMed Central for supplementary material.

Acknowledgments

We thank Kira Downey, Katherine Leehy, and Olivia Wicker for technical assistance. We also thank Michael Franklin for critical reading of this manuscript.

This work was supported by the NIH grants R01 CA159712 (CAL), K07 CA131501 (JHO), F32 CA210340 (THT), and T32 HL007741 (THT), ACS Institutional Research Grant #124166-IRG-58-001-52-IRG5 (JHO), Masonic Cancer Center, University of Minnesota, SP3 Award (CAL, JHO, KLS), and the National Center for Advancing Translational Sciences of the National Institutes of Health Award UL1TR000114 (JHO)

Author Manuscript Author Manuscript Author Manuscript Author Manuscript

References

1. Johnston SR. New strategies in estrogen receptor-positive breast cancer. Clin Cancer Res. 2010; 16(7):1979–87. [PubMed: 20332324]
2. Ma CX, Sanchez CG, Ellis MJ. Predicting endocrine therapy responsiveness in breast cancer. Oncology (Williston Park). 2009; 23(2):133–42. [PubMed: 19323294]
3. Musgrove EA, Sutherland RL. Biological determinants of endocrine resistance in breast cancer. Nat Rev Cancer. 2009; 9(9):631–43. [PubMed: 19701242]
4. Kato S, Endoh H, Masuhiro Y, Kitamoto T, Uchiyama S, Sasaki H, et al. Activation of the estrogen receptor through phosphorylation by mitogen-activated protein kinase. Science. 1995; 270(5241): 1491–4. [PubMed: 7491495]
5. Kato S. Estrogen receptor-mediated cross-talk with growth factor signaling pathways. Breast Cancer. 2001; 8(1):3–9. [PubMed: 11180760]
6. Need EF, Selth LA, Trotta AP, Leach DA, Giorgio L, O'Loughlin MA, et al. The unique transcriptional response produced by concurrent estrogen and progesterone treatment in breast cancer cells results in upregulation of growth factor pathways and switching from a Luminal A to a Basal-like subtype. BMC Cancer. 2015; 15:791. [PubMed: 26498662]
7. Girard BJ, Daniel AR, Lange CA, Ostrander JH. PELP1: a review of PELP1 interactions, signaling, and biology. Mol Cell Endocrinol. 2014; 382(1):642–51. [PubMed: 23933151]
8. Sareddy GR, Vadlamudi RK. PELP1: Structure, biological function and clinical significance. Gene. 2016; 585(1):128–34. [PubMed: 26997260]
9. Vadlamudi RK, Manavathi B, Balasenthil S, Nair SS, Yang Z, Sahin AA, et al. Functional implications of altered subcellular localization of PELP1 in breast cancer cells. Cancer Res. 2005; 65(17):7724–32. [PubMed: 16140940]
10. Castle CD, Cassimere EK, Denicourt C. LAS1L interacts with the mammalian Rix1 complex to regulate ribosome biogenesis. Mol Biol Cell. 2012; 23(4):716–28. [PubMed: 22190735]
11. Habashy HO, Powe DG, Rakha EA, Ball G, Macmillan RD, Green AR, et al. The prognostic significance of PELP1 expression in invasive breast cancer with emphasis on the ER-positive luminal-like subtype. Breast Cancer Res Treat. 2010; 120(3):603–12. [PubMed: 19495959]
12. Kumar R, Zhang H, Holm C, Vadlamudi RK, Landberg G, Rayala SK. Extranuclear coactivator signaling confers insensitivity to tamoxifen. Clin Cancer Res. 2009; 15(12):4123–30. [PubMed: 19470742]
13. Rajhans R, Nair HB, Nair SS, Cortez V, Ikuko K, Kirma NB, et al. Modulation of in situ estrogen synthesis by proline-, glutamic acid-, and leucine-rich protein-1: potential estrogen receptor autocrine signaling loop in breast cancer cells. Mol Endocrinol. 2008; 22(3):649–64. [PubMed: 18079323]
14. Daniel AR, Gaviglio AL, Knutson TP, Ostrander JH, D'Assoro AB, Ravindranathan P, et al. Progesterone receptor-B enhances estrogen responsiveness of breast cancer cells via scaffolding PELP1- and estrogen receptor-containing transcription complexes. Oncogene. 2015; 34(4):506–15. [PubMed: 24469035]
15. Cortez V, Samayoa C, Zamora A, Martinez L, Tekmal RR, Vadlamudi RK. PELP1 overexpression in the mouse mammary gland results in the development of hyperplasia and carcinoma. Cancer Res. 2014; 74(24):7395–405. [PubMed: 25377474]
16. Girard BJ, Regan Anderson TM, Welch SL, Nicely J, Seewaldt VL, Ostrander JH. Cytoplasmic PELP1 and ERRgamma protect human mammary epithelial cells from Tam-induced cell death. PLoS One. 2015; 10(3):e0121206. [PubMed: 25789479]
17. Girard BJ, Knutson TP, Kuker B, McDowell L, Schwertfeger KL, Ostrander JH. Cytoplasmic Localization of Proline, Glutamic Acid, Leucine-rich Protein 1 (PELP1) Induces Breast Epithelial Cell Migration through Up-regulation of Inhibitor of kappaB Kinase and Inflammatory Cross-talk with Macrophages. J Biol Chem. 2017; 292(1):339–50. [PubMed: 27881676]
18. Anzick SL, Kononen J, Walker RL, Azorsa DO, Tanner MM, Guan XY, et al. AIB1, a steroid receptor coactivator amplified in breast and ovarian cancer. Science. 1997; 277(5328):965–8. [PubMed: 9252329]

Author Manuscript Author Manuscript Author Manuscript Author Manuscript

19. Zheng FF, Wu RC, Smith CL, O'Malley BW. Rapid estrogen-induced phosphorylation of the SRC-3 coactivator occurs in an extranuclear complex containing estrogen receptor. Mol Cell Biol. 2005; 25(18):8273–84. [PubMed: 16135815]
20. Su Q, Hu S, Gao H, Ma R, Yang Q, Pan Z, et al. Role of AIB1 for tamoxifen resistance in estrogen receptor-positive breast cancer cells. Oncology. 2008; 75(3–4):159–68. [PubMed: 18827493]
21. Torres-Arzayus MI, Zhao J, Bronson R, Brown M. Estrogen-dependent and estrogen-independent mechanisms contribute to AIB1-mediated tumor formation. Cancer Res. 2010; 70(10):4102–11. [PubMed: 20442283]
22. Chang AK, Wu H. The role of AIB1 in breast cancer. Oncol Lett. 2012; 4(4):588–94. [PubMed: 23226788]
23. Knutson TP, Daniel AR, Fan D, Silverstein KA, Covington KR, Fuqua SA, et al. Phosphorylated and sumoylation-deficient progesterone receptors drive proliferative gene signatures during breast cancer progression. Breast Cancer Res. 2012; 14(3):R95. [PubMed: 22697792]
24. Holliday DL, Speirs V. Choosing the right cell line for breast cancer research. Breast Cancer Res. 2011; 13(4):215. [PubMed: 21884641]
25. Horwitz KB, Mockus MB, Lessey BA. Variant T47D human breast cancer cells with high progesterone-receptor levels despite estrogen and antiestrogen resistance. Cell. 1982; 28(3):633–42. [PubMed: 7200400]
26. Wu RC, Qin J, Yi P, Wong J, Tsai SY, Tsai MJ, et al. Selective phosphorylations of the SRC-3/AIB1 coactivator integrate genomic reponses to multiple cellular signaling pathways. Mol Cell. 2004; 15(6):937–49. [PubMed: 15383283]
27. Foekens JA, Look MP, Peters HA, van Putten WL, Portengen H, Klijn JG. Urokinase-type plasminogen activator and its inhibitor PAI-1: predictors of poor response to tamoxifen therapy in recurrent breast cancer. J Natl Cancer Inst. 1995; 87(10):751–6. [PubMed: 7563153]
28. Meijer-van Gelder ME, Look MP, Peters HA, Schmitt M, Brunner N, Harbeck N, et al. Urokinase-type plasminogen activator system in breast cancer: association with tamoxifen therapy in recurrent disease. Cancer Res. 2004; 64(13):4563–8. [PubMed: 15231667]
29. Gyorffy B, Lanczky A, Eklund AC, Denkert C, Budczies J, Li Q, et al. An online survival analysis tool to rapidly assess the effect of 22,277 genes on breast cancer prognosis using microarray data of 1,809 patients. Breast Cancer Res Treat. 2010; 123(3):725–31. [PubMed: 20020197]
30. Schulenburg A, Blatt K, Cerny-Reiterer S, Sadovnik I, Herrmann H, Marian B, et al. Cancer stem cells in basic science and in translational oncology: can we translate into clinical application? J Hematol Oncol. 2015; 8:16. [PubMed: 25886184]
31. Czerwinska P, Kaminska B. Regulation of breast cancer stem cell features. Contemp Oncol (Pozn). 2015; 19(1A):A7–A15. [PubMed: 25691826]
32. Lathia JD, Liu H. Overview of Cancer Stem Cells and Stemness for Community Oncologists. Target Oncol. 2017; 12(4):387–99. [PubMed: 28664387]
33. Grimshaw MJ, Cooper L, Papazisis K, Coleman JA, Bohnenkamp HR, Chiapero-Stanke L, et al. Mammosphere culture of metastatic breast cancer cells enriches for tumorigenic breast cancer cells. Breast Cancer Res. 2008; 10(3):R52. [PubMed: 18541018]
34. Ginestier C, Hur MH, Charafe-Jauffret E, Monville F, Dutcher J, Brown M, et al. ALDH1 is a marker of normal and malignant human mammary stem cells and a predictor of poor clinical outcome. Cell Stem Cell. 2007; 1(5):555–67. [PubMed: 18371393]
35. Song X, Chen J, Zhao M, Zhang C, Yu Y, Lonard DM, et al. Development of potent small-molecule inhibitors to drug the undruggable steroid receptor coactivator-3. Proc Natl Acad Sci U S A. 2016; 113(18):4970–5. [PubMed: 27084884]
36. Torres-Arzayus MI, Font de Mora J, Yuan J, Vazquez F, Bronson R, Rue M, et al. High tumor incidence and activation of the PI3K/AKT pathway in transgenic mice define AIB1 as an oncogene. Cancer Cell. 2004; 6(3):263–74. [PubMed: 15380517]
37. Torres-Arzayus MI, Yuan J, DellaGatta JL, Lane H, Kung AL, Brown M. Targeting the AIB1 oncogene through mammalian target of rapamycin inhibition in the mammary gland. Cancer Res. 2006; 66(23):11381–8. [PubMed: 17145884]

Author Manuscript Author Manuscript Author Manuscript Author Manuscript

38. Louie MC, Zou JX, Rabinovich A, Chen HW. ACTR/AIB1 functions as an E2F1 coactivator to promote breast cancer cell proliferation and antiestrogen resistance. Mol Cell Biol. 2004; 24(12): 5157–71. [PubMed: 15169882]
39. Zhao W, Zhang Q, Kang X, Jin S, Lou C. AIB1 is required for the acquisition of epithelial growth factor receptor-mediated tamoxifen resistance in breast cancer cells. Biochem Biophys Res Commun. 2009; 380(3):699–704. [PubMed: 19285025]
40. Osborne CK, Bardou V, Hopp TA, Chamness GC, Hilsenbeck SG, Fuqua SA, et al. Role of the estrogen receptor coactivator AIB1 (SRC-3) and HER-2/neu in tamoxifen resistance in breast cancer. J Natl Cancer Inst. 2003; 95(5):353–61. [PubMed: 12618500]
41. Percharde M, Lavial F, Ng JH, Kumar V, Tomaz RA, Martin N, et al. Ncoa3 functions as an essential Esrrb coactivator to sustain embryonic stem cell self-renewal and reprogramming. Genes Dev. 2012; 26(20):2286–98. [PubMed: 23019124]
42. Rohira AD, Yan F, Wang L, Wang J, Zhou S, Lu A, et al. Targeting SRC Coactivators Blocks the Tumor-Initiating Capacity of Cancer Stem-like Cells. Cancer Res. 2017; 77(16):4293–304. [PubMed: 28611048]
43. Park H, Lee S, Shrestha P, Kim J, Park JA, Ko Y, et al. AMIGO2, a novel membrane anchor of PDK1, controls cell survival and angiogenesis via Akt activation. J Cell Biol. 2015; 211(3):619–37. [PubMed: 26553931]
44. Choi EJ, Kim DH, Kim JG, Kim DY, Kim JD, Seol OJ, et al. Estrogen-dependent transcription of the NEL-like 2 (NELL2) gene and its role in protection from cell death. J Biol Chem. 2010; 285(32):25074–84. [PubMed: 20538601]
45. Duffy MJ, McGowan PM, Harbeck N, Thomssen C, Schmitt M. uPA and PAI-1 as biomarkers in breast cancer: validated for clinical use in level-of-evidence-1 studies. Breast Cancer Res. 2014; 16(4):428. [PubMed: 25677449]
46. Mebarki S, Desert R, Sulpice L, Sicard M, Desille M, Canal F, et al. De novo HAPLN1 expression hallmarks Wnt-induced stem cell and fibrogenic networks leading to aggressive human hepatocellular carcinomas. Oncotarget. 2016; 7(26):39026–43. [PubMed: 27191501]
47. Liu Y, Nenutil R, Appleyard MV, Murray K, Boylan M, Thompson AM, et al. Lack of correlation of stem cell markers in breast cancer stem cells. Br J Cancer. 2014; 110(8):2063–71. [PubMed: 24577057]
48. Ravindranathan P, Lee TK, Yang L, Centenera MM, Butler L, Tilley WD, et al. Peptidomimetic targeting of critical androgen receptor-coregulator interactions in prostate cancer. Nat Commun. 2013; 4:1923. [PubMed: 23715282]
49. Cortez V, Mann M, Tekmal S, Suzuki T, Miyata N, Rodriguez-Aguayo C, et al. Targeting the PELP1-KDM1 axis as a potential therapeutic strategy for breast cancer. Breast Cancer Res. 2012; 14(4):R108. [PubMed: 22812534]
50. Gonugunta VK, Sareddy GR, Krishnan SR, Cortez V, Roy SS, Tekmal RR, et al. Inhibition of mTOR signaling reduces PELP1-mediated tumor growth and therapy resistance. Mol Cancer Ther. 2014; 13(6):1578–88. [PubMed: 24688046]
51. Bozorgi A, Khazaei M, Khazaei MR. New Findings on Breast Cancer Stem Cells: A Review. J Breast Cancer. 2015; 18(4):303–12. [PubMed: 26770236]

Author Manuscript Author Manuscript Author Manuscript Author Manuscript

Implications

These data demonstrate that cytoplasmic PELP1/AIB1 containing complexes function to promote advanced cancer phenotypes, including outgrowth of stem-like cells, associated with estrogen-independent breast cancer progression.

Author Manuscript Author Manuscript Author Manuscript Author Manuscript

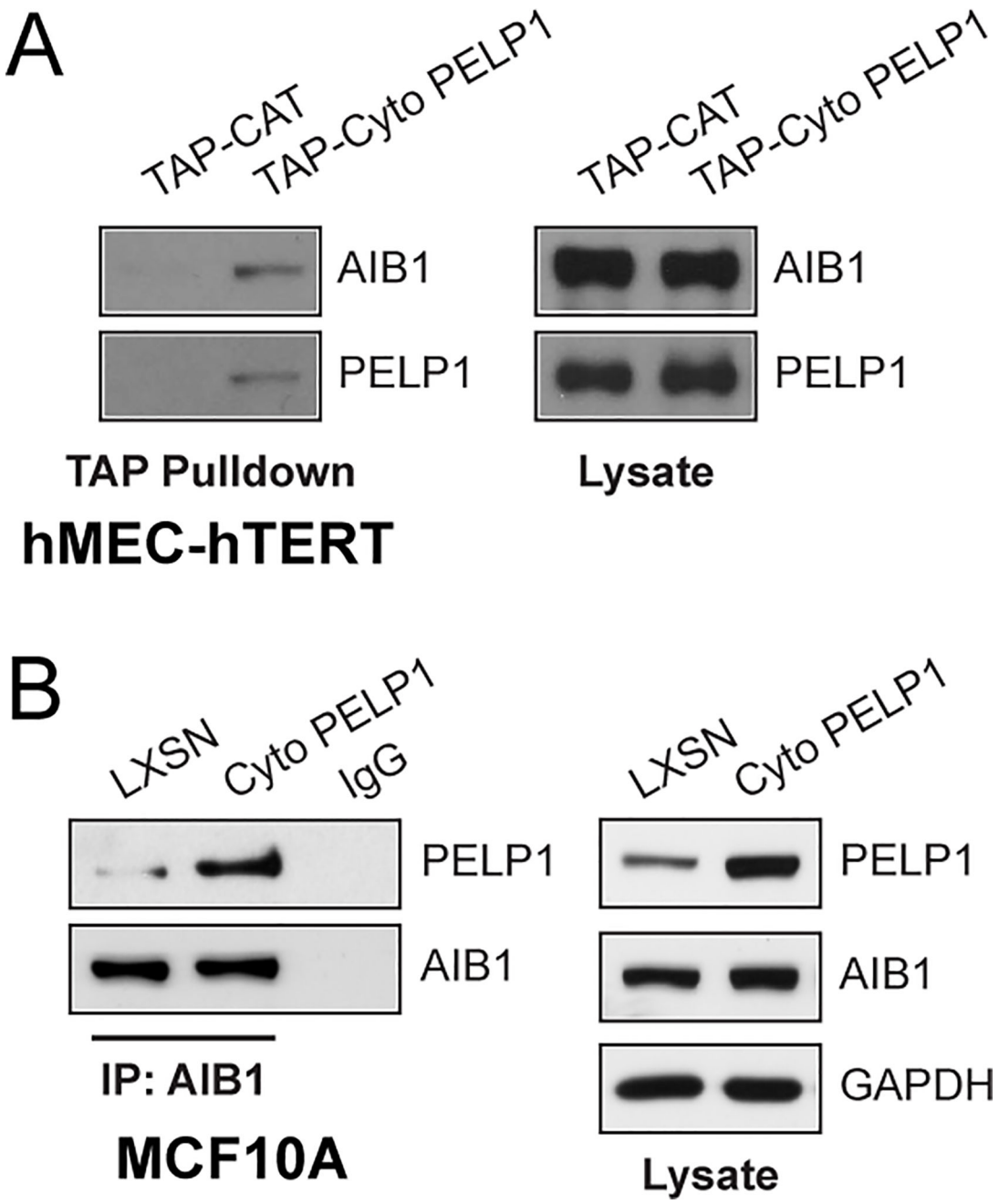

Figure 1.

AIB1 interacts with cytoplasmic PELP1. (**A**) Western blot of TAP pull-down (left) and whole cell lysates (right) in hTERT mammary epithelial cells. (**B**) Western blot showing co-immunoprecipitation (left) and whole cell lysates (right) of PELP1 and AIB1 in MCF10A cells.

Author Manuscript Author Manuscript Author Manuscript Author Manuscript

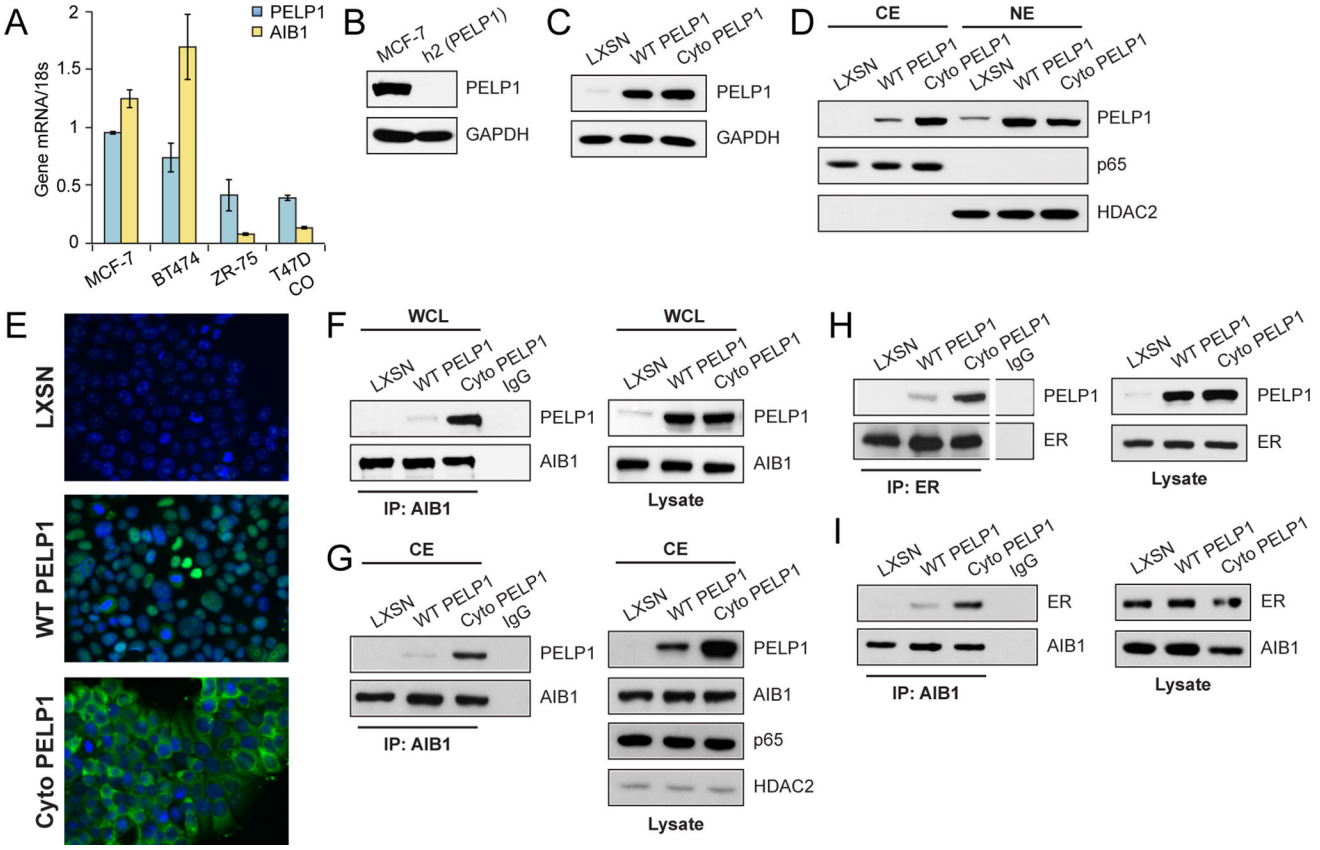

Figure 2.

Generation of PELP1 models in SR+ breast cancer cells. (**A**) mRNA levels of PELP1 and AIB1 in a panel of luminal breast cancer lines. Graphed data represents the mean ± SD (n = 3). (**B**) Western blot showing knockdown of endogenous PELP1 in MCF-7 cells (h2 MCF-7) using a double nickase approach. (**C**) Western blot showing overexpression of PELP1 in LXSN (vector control), WT PELP1, and cyto PELP1 in h2 MCF-7 PELP1 cells. (**D**) Western blot showing PELP1 expression in cellular fractionation (CE, cytoplasmic extract; NE, nuclear extract) from h2 MCF-7 PELP1 cells. p65 and HDAC2 (loading controls). (**E**) Immunofluorescence in h2 MCF-7 PELP1 cells. DAPI; blue. Western blot showing co-immunoprecipitation (left) and whole cell lysates (right) of (**F**) PELP1 and AIB1, (**H**) PELP1 and ER, and (**I**) ER and AIB1 in h2 MCF-7 PELP1 cells (under basal conditions). (**G**) Western blot showing co-immunoprecipitation from cytoplasmic extract (left) and cytoplasmic extract (right) of PELP1 and AIB1 (under basal conditions).

Author Manuscript Author Manuscript Author Manuscript Author Manuscript

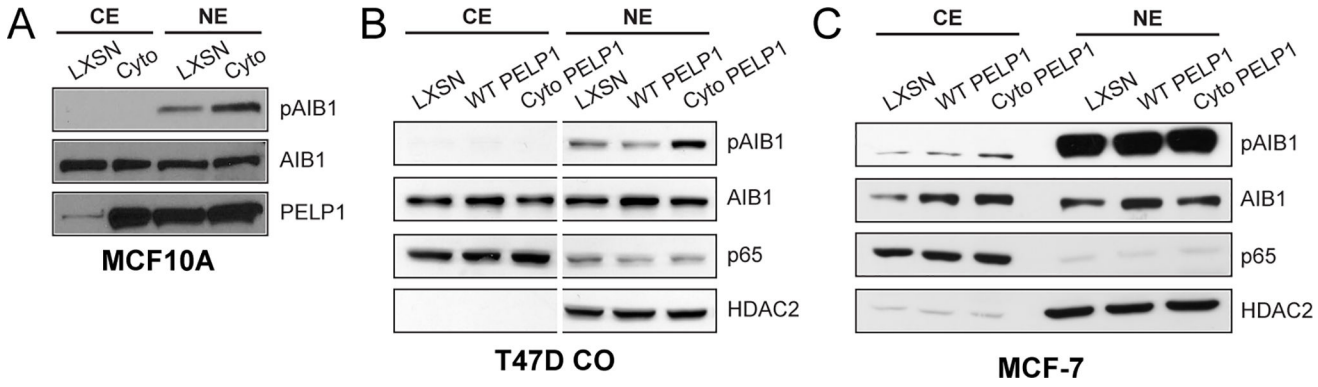

Figure 3.

AIB1 activation (pThr24) levels are altered in the presence of cytoplasmic PELP1. Cellular fractionation in mammary epithelial cells (**A**) MCF10A and breast cancer cells (**B**) T47D CO and (**C**) MCF-7. Western blots show phosphorylated (pAIB1; Thr24) and total AIB1.

Author Manuscript Author Manuscript Author Manuscript Author Manuscript

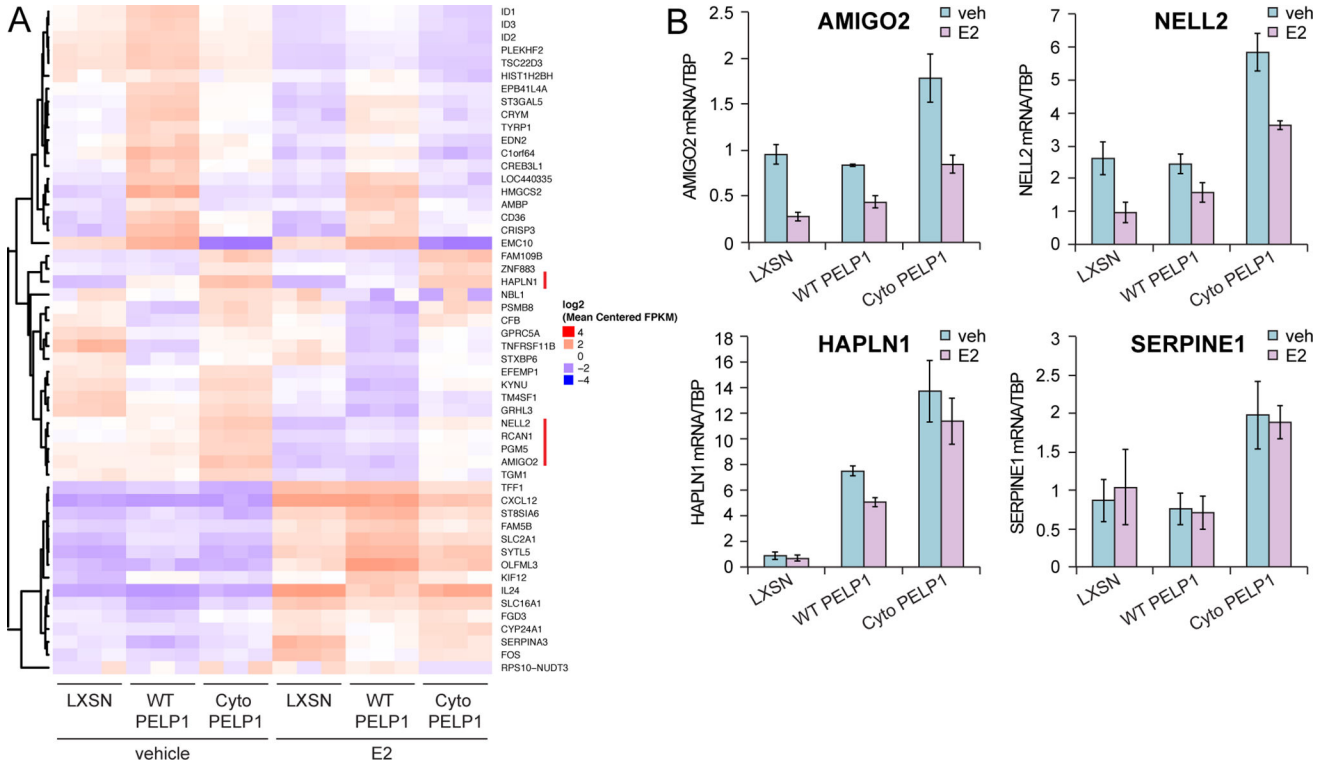

Figure 4.

Cytoplasmic PELP1-induced gene expression in h2 MCF-7 PELP1 models. (**A**) Supervised heat map of differentially expressed genes in h2 MCF-7 PELP cells (LXSN, WT PELP1, and cyto PELP1). Cells were treated with vehicle (EtOH) or E2 (1 nM) for 6 h. Genes were hierarchically clustered using average clustering method and Pearson correlation as distance in R ComplexHeatmap package (PMID: 27207943). The columns are grouped by experimental condition and biological replicates for display purposes. (**B**) qRT-PCR validation of select genes from RNA-Seq analysis in h2 MCF-7 PELP1 cells. Graphed data represents the mean ± SD (n = 3).

Author Manuscript Author Manuscript Author Manuscript Author Manuscript

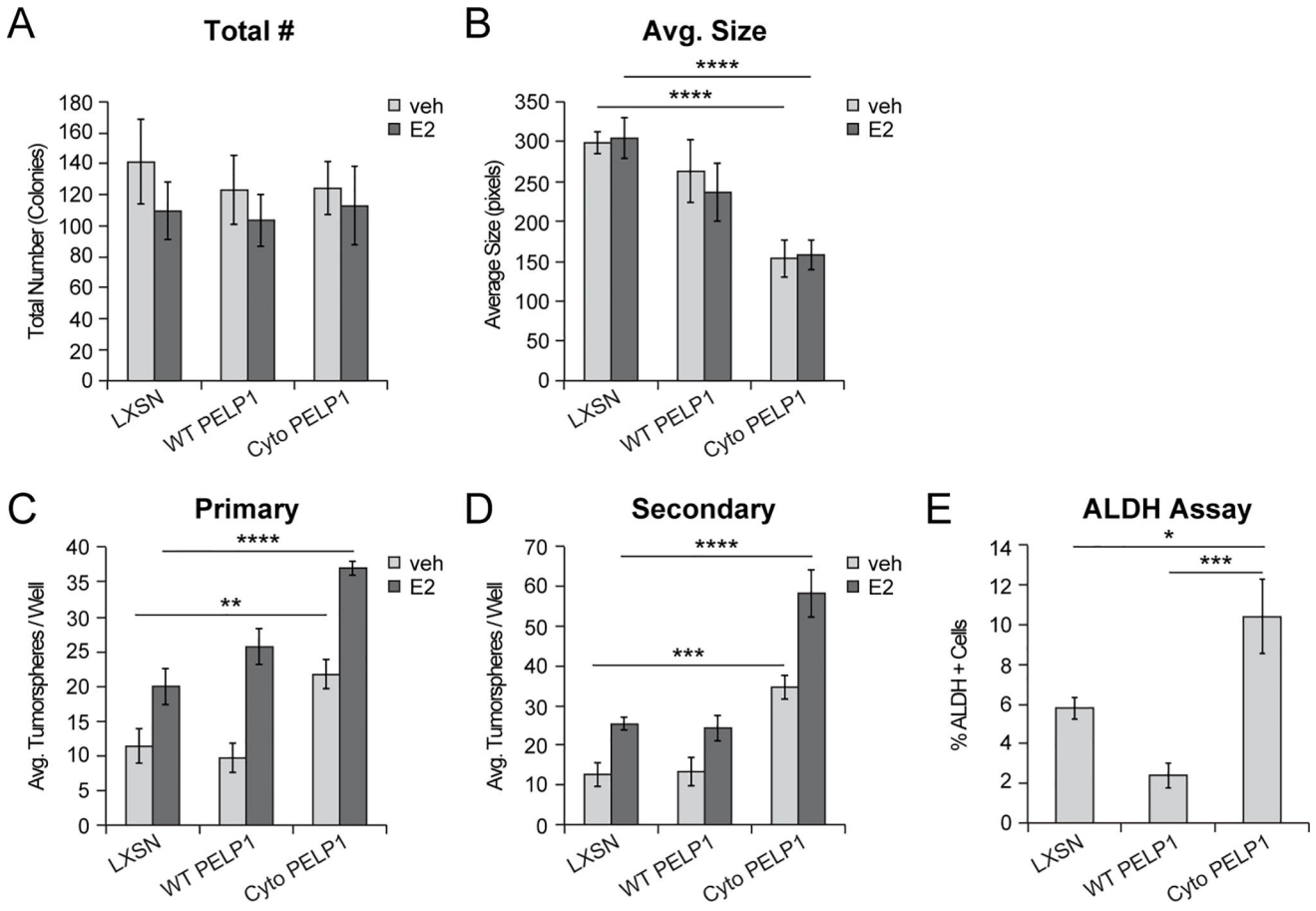

Figure 5.

Cytoplasmic PELP1 promotes tumorsphere formation in breast cancer cells. (**A,B**) Soft agar colony formation in h2 MCF-7 PELP1 cells (LXSN, WT PELP1, or cyto PELP1). Cells were grown in vehicle (EtOH) or E2 (1 nM). Soft agar data were analyzed in terms of (**A**) total number of colonies and (**B**) average colony size. (**C**) Primary and (**D**) secondary tumorspheres in h2 MCF-7 PELP1 cells (LXSN, WT PELP1, or cyto PELP1). Cells were treated with vehicle (EtOH) or E2 (1 nM). (**E**) ALDH activity in primary tumorspheres formed from h2 MCF-7 PELP1 cells was assessed using flow cytometry. Graphed data represents the mean ± SD (n = 3). ** $p < 0.01$, *** $p < 0.001$, **** $p < 0.0001$

Author Manuscript Author Manuscript Author Manuscript Author Manuscript

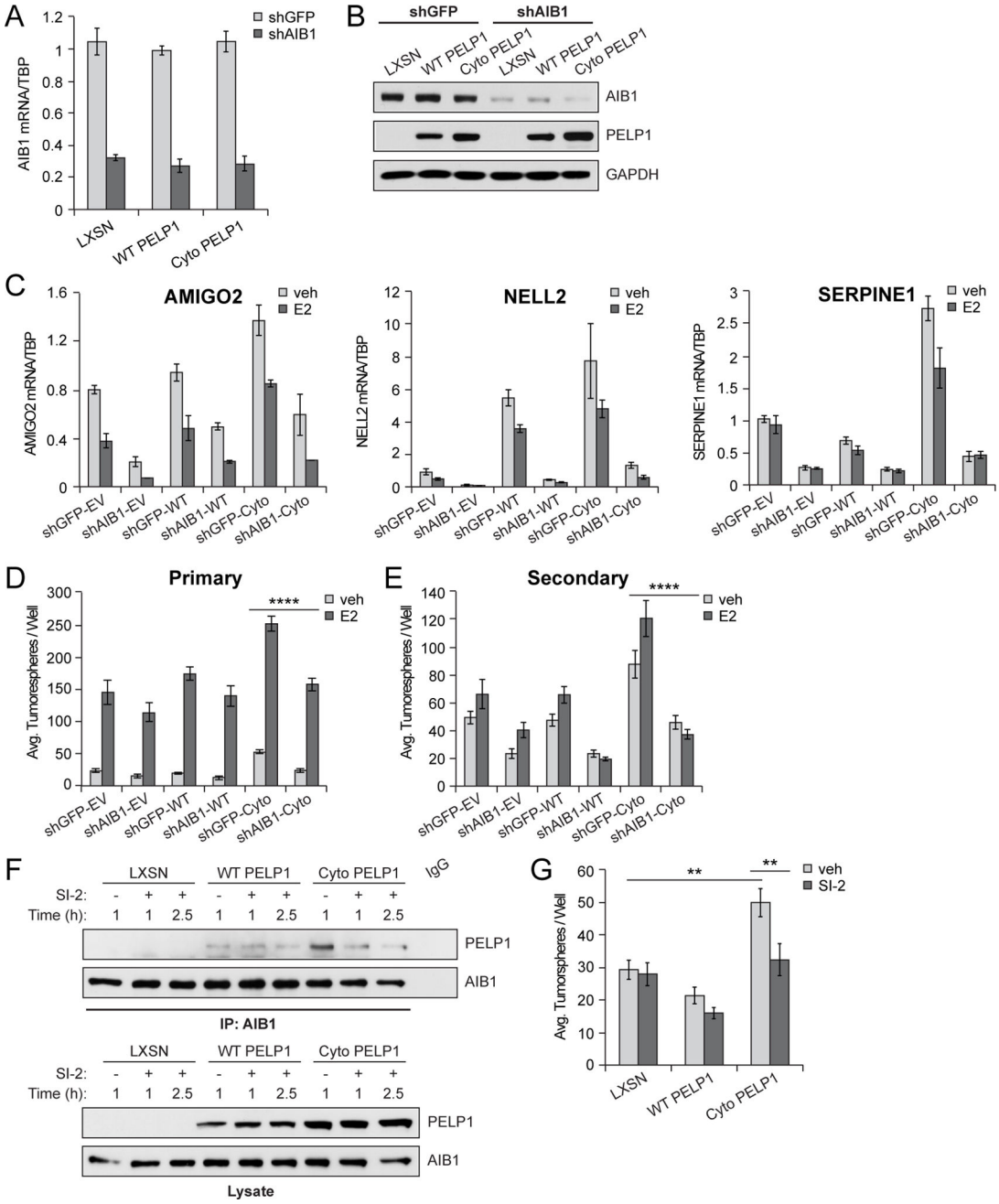

Figure 6.

AIB1 knockdown affects cancer cell biology phenotypes in PELP1 models. (**A**) mRNA and (**B**) Western blot showing AIB1 knockdown in h2 MCF-7 PELP1 models. (**C**) mRNA levels of genes (e.g. *SERPINE1*, *AMIGO2*, *NELL2*) identified from our RNA-Seq analysis in AIB1 knockdown h2 MCF-7 PELP1 models. (**D**) Primary and (**E**) secondary tumorspheres in AIB1 knockdown h2 MCF-7 PELP1 models. Cells were treated with vehicle (EtOH) or E2 (1 nM). (**F**) Western blot showing co-immunoprecipitation (top) and whole cell lysates (bottom) of PELP1 and AIB1 in h2 MCF-7L PELP1 cells treated with vehicle (DMSO) or SI-2 (100 nM). (**G**) Primary tumorspheres in h2 MCF-7L PELP1 cells overexpressing

LXSN, WT PELP1, or cyto PELP1 treated with vehicle (DMSO) or SI-2 (100 nM). Graphed data represents the mean ± SD (n = 3). ** $p < 0.01$, **** $p < 0.0001$.

Author Manuscript Author Manuscript Author Manuscript Author Manuscript

Author Manuscript Author Manuscript Author Manuscript Author Manuscript

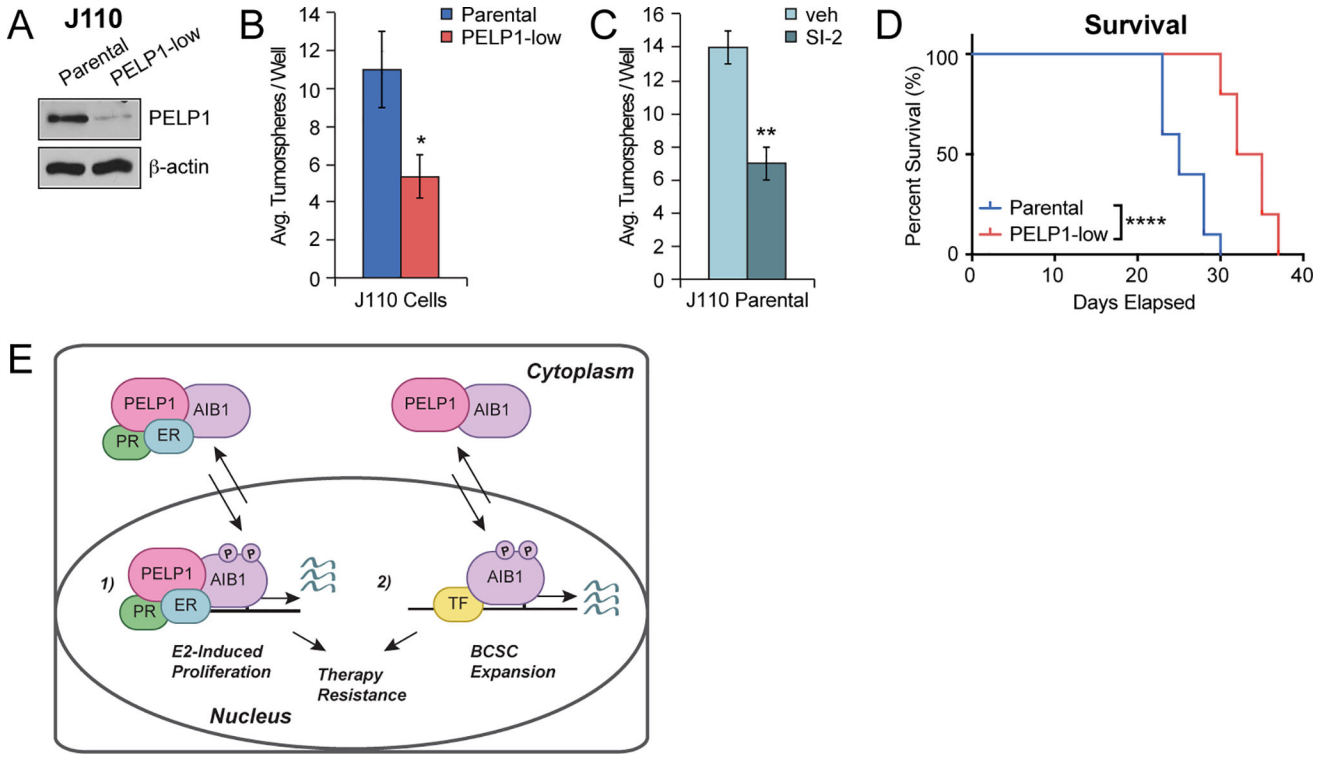

Figure 7.

PELP1 knockdown prolongs survival time in mice transplanted with MMTV-AIB1 tumor cells. (**A**) Western blot showing knockdown of endogenous PELP1 in J110 mouse tumor cells (PELP1-low) using a double nickase approach. (**B**) Primary tumorspheres in J110 (parental or PELP1-low) cells. (**C**) Primary tumorspheres in J110 parental cells treated with vehicle (DMSO) or SI-2 (100 nM). Graphed data represents the mean ± SD (n = 3). * $p < 0.05$, ** $p < 0.01$ (Student *t* test). (**D**) Kaplan-Meier survival curve. J110 cells (parental or PELP1-low) were transplanted into recipient FVB mice (10 mice/group). Data represent two independent trials. **** $p < 0.0001$. (**E**) Model for cytoplasmic PELP1 signaling in SR+ breast cancer models. 1) PELP1/ER/PR/AIB1 complexes regulate E2-induced genes that promote proliferation and therapy endocrine therapy resistance (14). 2) Cytoplasmic PELP1 promotes AIB1 phosphorylation independent of E2 and ER, which results in regulation of genes, via yet to be identified transcription factors (TFs) that promote breast cancer stem cell (BCSC) survival and/or expansion.